MOEMS Based Laser Scanning Device for Light-Driven Microfluidics

Andreas Tortschanoff[1], Diana Damian[2], Matthias Kremer[3]

[1,2,3]Carinthian Tech Research AG, Europastrasse 12, 9524 Villach, Austria

([1]andreas.tortschanoff@ctr.at)

Abstract- In this paper we present our laser scanning device, where control of the laser focus was achieved using MOEMS-technology. This offers the possibility for a compact and easy to use variable focus scanning device. First experiments were performed with the device, where laser controlled thermally induced flows were used to move polystyrene beads in an unstructured microfluidic cell, which demonstrates the capability of the device in the field of light-driven microfluidics.

Keywords- *MOEMS, laser-scanner, tunable lens, light driven microfluidics*

I. INTRODUCTION

In the field of microfluidics and lab-on-a-chip experiments one of the challenges consists in having the ability to remotely manipulate fluids, droplets and particles. Light-driven microfluidics [1] provides one way of accomplishing this challenge by using laser light in order to actuate fluids. A well-chosen light source has the capability to create optical forces that can have highly selective action (e.g. optical tweezers) or, less specifically, to deposit energy in the liquid and to induce thermal flows in the sample solution (e.g. for the manipulation of particles) or to start chemical reactions at specific locations. In all cases, these processes are contactless and sterile which is an important advantage for medical, chemical and biological applications.

From the technical point of view, it is important to have high accuracy and precise control of position and shape of the focal spot inside a fluid. The device presented in this paper relies on MOEMS elements to be combined with Lab-on-a-Chip technology. Both technologies have a wide range of applications from biotechnology and medicine to communication and inertial sensing. Used together they offer the possibility to develop a compact and easy to use device that serves for several types of laboratory experiments.

The scanner device should meet the following constraints. First, the setup should be compact in all dimensions. Second, we want a high power density in the focus, thus the spot size should be reasonably small over the whole 3D volume of interest. The latter should have lateral dimensions in the range of several millimeters, in order to be able to cover the whole

(or at least a large part of the) microfluidic cell. Furthermore, placement of the laser-spot should be fast, on the order of ten milliseconds or less and the device should be controlled via a computer interface and be easy to operate.

The system design was performed considering these constraints. Hence, the device was set up with the laser source, an optional beam expander, the tunable lens and the micro-mirror. To maintain compactness, the use of additional lens systems was mostly avoided.

In the following we present the system and show first experimental results.

II. GENERAL CONSIDERATIONS

The general concept is shown in **Error! Reference source not found.**. Basically a laser output (A) can be adjusted in size by a telescope (B) and, subsequently, is focused with a tunable lens (C) before passing the MOEMS scanner mirror (D), which deflects the light to an arbitrary position on the microfluidic cell (E). The novel key components are the MOEMS scanner mirror and the tunable lens. Both are electrically controlled and allow very fast and accurate positioning and refocusing of the laser spot. Different laser sources can be used with the scanner device. The setup is computer controlled.
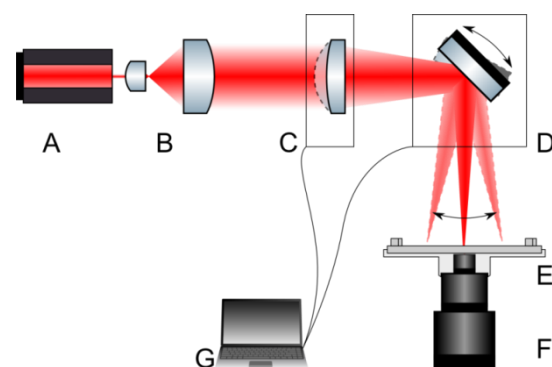

Figure 1. Schematic layout; A:laser, B:beam expander, C:tunable lens, D:MOEMS mirror, E:microfluidic chip on sample holder, F:microscope, G:computer.

A. Mathematical description

To describe the laser scanning system mathematically, we used the following definitions: The tilting angles of the micro mirror are referred to as ξ and η for tilting around the y and x axis, respectively. The deflection angles of the beam are referred to as α and β regarding the deflection around the x and y axis, respectively. The focal length of the tunable lens is called f. The origin of the optical axis z is set to the center of the micro mirror. Thus, the location of the laser spot can be described with the scanner coordinates (ξ, η, f). To transform real-world coordinates (x, y, z) of a desired spot location into scanner coordinates, the following calculations need to be performed.
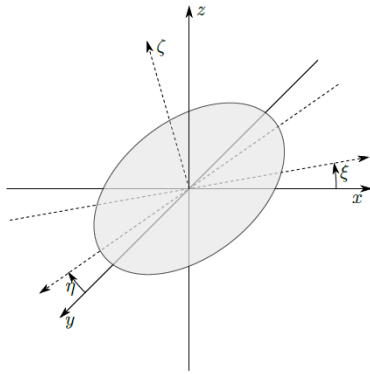

Figure 2. Axes and angles at the micromirror

The angles of reflection are dependent on the tilting angles of the mirror. For small tilting angles, the reflection angles are independent of each other and can be approximated by

$$\alpha = 2\xi$$
$$\beta = 2\eta. \tag{1}$$

Thus, the required reflection angles for a desired spot location can be expressed as

$$\Delta x = z \cdot \tan(2\alpha)$$
$$\Rightarrow \alpha = \tfrac{1}{2}\arctan\left(\tfrac{x}{z}\right) \tag{2}$$
$$\beta = \tfrac{1}{2}\arctan\left(\tfrac{y}{z}\right)$$

with the distance z between the micro mirror and the spot plane and the displacement of the focal point from the initial position Δx and Δy. Therefore, the transformation of tilting angles and focal length to spot location is

$$\begin{pmatrix} \xi \\ \eta \\ f \end{pmatrix} = \begin{pmatrix} \tfrac{1}{2}\alpha \\ \tfrac{1}{2}\beta \\ f \end{pmatrix} = \begin{pmatrix} \tfrac{1}{2}\arctan\left(\tfrac{x}{z}\right) \\ \tfrac{1}{2}\arctan\left(\tfrac{y}{z}\right) \\ l_1 + \sqrt{x^2 + y^2 + z^2} \end{pmatrix} \tag{3}$$

with l_1, the offset distance between the tunable lens and the micro mirror. This shows, that the focal spot can be set to any arbitrary point in a univocal way within a three dimensional working space by setting the focal length of the tunable lens

and the tilting angles of the micro mirror and the relation between internal and external coordinates is given by (3).

B. Diffraction limited resolution

There are fundamental limitations to the smallest spot size achievable with focusing optics. As laser radiation propagates with an inhomogeneous intensity distribution across the beam cross shape, the beam cannot be focused to an arbitrary small point. In the case of a mode zero laser source, the approximation of a Gaussian shaped intensity distribution – a so called Gaussian beam – of the beam is applicable. The diffraction limited focal radius for a Gaussian beam is dependent on the wavelength, the focal length and the effective aperture of the optical system. If the beam is collimated and the diameter matches the lens's aperture, the smallest focal radius calculates as

$$\omega_0' = \frac{\lambda f}{\pi \omega_0} \tag{4}$$

with wavelength λ, focal length f and lens radius ω_0 [4]. A commonly used quantity is the Rayleigh length z_R, which is defined as the distance from the focal point along the optical axis, where the area of the cross section has doubled.

$$z_R = \frac{\pi \omega_0'^2}{\lambda} \tag{5}$$

Figure 3 shows the correlations of focal length and beam diameter for a collimated Gaussian beam travelling through a lens. After the beam waist, which is at the focal point, the beam propagates with the divergence angle $\theta = \frac{\lambda}{\pi \omega_0'}$ [4]. This shows that in order to achieve a small spot size, a large beam and a small focal length are desirable. In our geometry, the beam diameter is limited either by the lens aperture or the MOEMS mirror diameter.
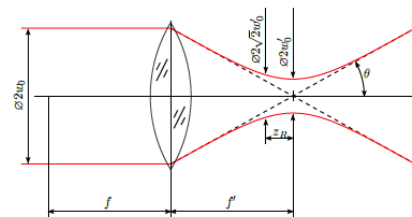

Figure 3. Diffraction limited focal radius of a Gaussian beam. When a collimated beam with a diameter 2w0 travels through a focusing lens, the minimum beam diameter $2\omega_0'$ is achieved at the focal length f' of the lens. The Rayleigh length zR is the distance from the focal point, where the beam cross section area has doubled. θ is the divergence angle.

C. Optical Simulation

A ray tracing simulation was executed using Variant Zemax. The model of the tunable lens was supplied by the manufacturers. Figure 4 shows screen-shots from the simulation-tool with the optimized setup for a wavelength of $\lambda = 650$ nm. The different colors of the beams correspond to different focal lengths and deflection angles, respectively.
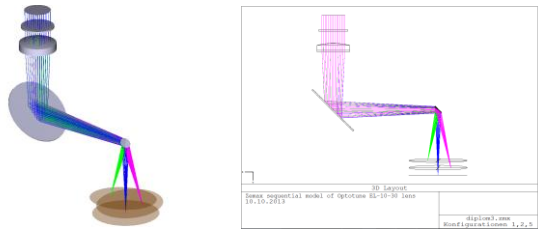
Figure 4. Ray tracing simulation of the optical setup. (a) 2D side view, (b) 3D perspective view. Wavelength l=650 nm. The different colors of the beams correspond to different focal lengths and deflection angles. (blue: f=150 mm, a=0°, b=0°; green: f=145 mm, a=4°, b=4°, red: f=147.5 mm, a=-4°, b=4°)

Based on the simulation results, the optical setup was optimized, regarding the distances between components, to achieve the desired working parameters. The optimized setup is free of clipping when using the maximum aperture, which is restricted by the diameters of the micro-mirror and of the tunable lens.

III. SETUP

Our MOEMS based laser scanner device features an electrically tunable lens for adjusting the focal length of the laser beam and an electrostatically driven quasi-static MOEMS micro-mirror for precise beam steering (see Figure 1). Typically a 650 nm laser diode with an optical power of 13 mW was used but other laser sources were tested as well. Spot-sizes below 100 μm were achieved. **Error! Reference source not found.** shows a photo of the experimental setup.
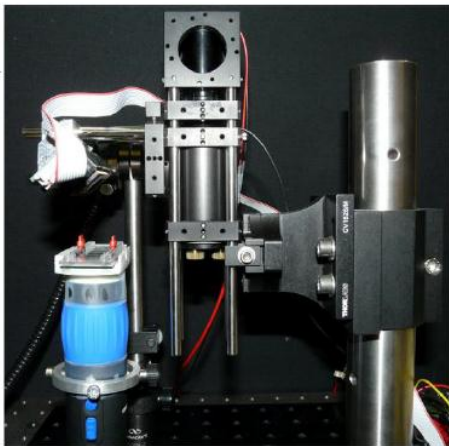

Figure 5. Photo of the microfluidic demonstrator experiment

This device features high flexibility, and, due to absence of large mechanical movements, it is highly robust and has low power consumption. This property represents an important asset, when thinking about portable devices.

A. Description and Characterization of the Key Components

1) Micromirror S0364DB

The MOEMS mirror used is manufactured by MirrorcleTech, CA. Its mirror plate has a diameter of 3.2mm and is gimbal-less mounted. It is quasi static dual axis driven with electrostatic actuators [3].
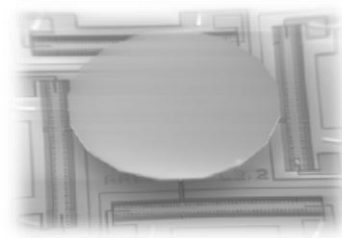

Figure 6. Photograph of a gimbal less mounted micromirror.

a) Characterization

The micro mirror's tilting characteristics according to the applied voltages were measured with the calibration camera. A focused beam was guided towards the micro mirror and deflected onto the camera chip, which was placed on the focal plane. As the distance between the mirror and the camera, as well as the camera chip's pixel size were known, the tilting angle could be calculated by a trigonometric approach, according to (3). **Error! Reference source not found.** shows the tilting angles versus the applied voltage at a bias of 38 V. As expected, the tilting angles depend on the applied voltages in a nearly linear manner.
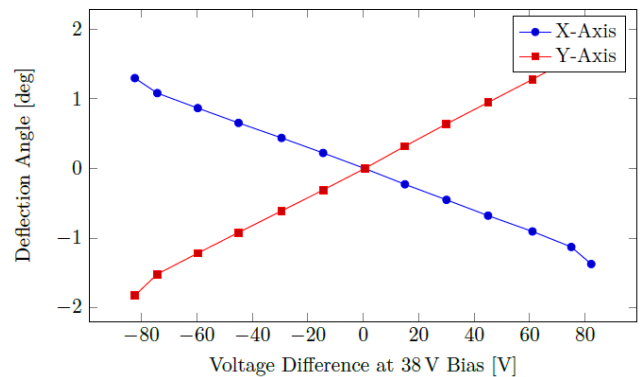

Figure 7. Mechanical deflection of the micro mirror vs. applied voltage with 38 V bias. The tilting angle is to a good approximation linear.

2) Tunable Lens

The tunable lens [2] (Optotune EL-10-30), which was used in this work, is based on the mechanical stressing principle. It consists of a lens, which has one fixed surface and one flexible membrane to form the second surface. The volume in between the surfaces is filled with a highly transparent polymer fluid. With a ring-shaped electromagnetic actuator, pressure can be applied to the outer region of the lens body, which results in a movement of the fluid towards the inner region of the lens and, therefore, in an expansion of the lens shape. As the lens shape is plano-convex, expansion of the lens shape is equal to an reduction of the lens curvature radius, thus, to a shortening of the focal length. Due to the flexibility of the membrane, a deformation of the lens cannot be avoided, when operated horizontally. To avoid resulting aberration, on construction of the optical setup one should arrange the tunable lens vertically. The electro-magnetic actuator is current driven, which makes the focal length of the lens continuously adjustable in between

these two limits. Tuning of the current is realized via a computer interface.

a) Characterization

To determine the current dependency of the lens's focal length, a test setup was build, on which the focal length was measured. The lens was put on a linear rail, together with a screen, which was mounted to a slide. While applying a current, which was tuned from 300mA to 0 mA, the slide was slid along the rail and the throw for the smallest spot size was measured. **Error! Reference source not found.** shows the data, acquired with this method. The measured working range is 52 mm to 150 mm. The dependency of the focal length from the current was expected to be linear. However, it turned out a parabola fit the actual measured data much better. In addition, when tuning the current from 0mA to 300 mA, a hysteresis was noticed. A compensation of this hysteresis was implemented into the driver software.
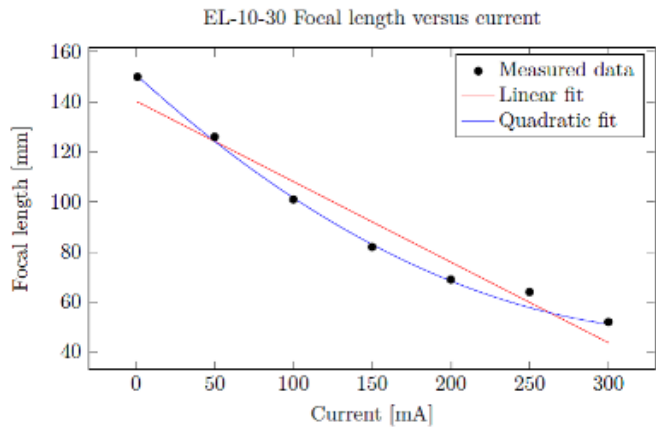

Figure 8. Experimental data for the EL-30-10 lens. Focal length vs. applied current. Two trend lines are fitted, one regarding the expected linear dependence and one with a quadratic polynomial function, which tends to deliver better results.

3) Laser Sources

Different laser sources were used with the scanner device. A HeNe laser with high beam quality was used for characterization of the micro-mirror and the tunable lens, as well as for calibration of the experimental setup. Different diode laser modules with higher output power, (but lower beam quality), were mainly used for the experiments.

TABLE I. COMPARISON OF DIFFERENT LASER SOURCES, ACCORDING TO WAVELENGTH L, DIFFRACTION LIMITED SPOT SIZE A_{THEO}, MEASURED SPOT SIZE A_{MEAS}, AND THE CORRESPONDING RAYLEIGH LENGTHS Z_{RTHEO} AND Z_{RMEAS}. MEASUREMENTS TAKEN AT A FOCAL LENGTH OF F = 120 MM.

Parameter	HeNe-Laser	RLDG650-13-3
λ [nm]	633	650
P [mW]	1	13
A_{theo} [μm²]	73	77
A_{meas} [μm²]	57	1360
z_{Rtheo} [μm]	115	118
z_{Rmeas} [μm]	278	906

Typical parameters are shown in Table I. In addition there is the possibility of fiber coupled input.

IV. DEMONSTRATION EXPERIMENTS

Demonstration experiments were performed in a microfluidic chip containing unstructured chambers with dimensions of 2.6×10×0.2mm³. Observation of the experiments in the microfluidic cell was realized with a digital microscope.

To demonstrate the feasibility of light-driven microfluidics with our device, we performed two demonstration experiments. In the first experiment, it was shown, that the laser-power is sufficient to achieve boiling in the liquid, which perturbs the laminar flow in the cell. In a second experiment we showed, that, it is possible to find conditions where thermal flows are induced in the microfluidic systems, which can be used to manipulate micrometer sized particles
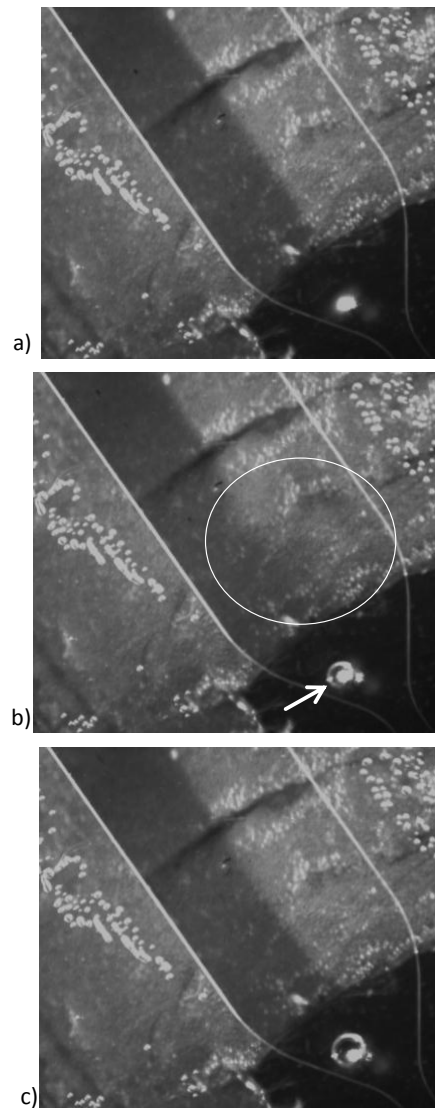

Figure 9. Shockwave in a laminar flow: a) Situation when the laser spot is turned on. b) Creation of a bubble generates a shock wave, which perturbs the laminar flow. c) The bubble further expands and stays centered at the laser focus until the laser is turned off.

A. Shockwave in a laminar flow

This is shown in Fig. 2. Fig. 2a shows the initial situation where one can see a laminar two-phase flow in the flow cell. The solvent in this case is water and in the left channel a dye was added in order to increase the absorption of the laser and to visualize the liquid flow. Fig. 2b shows the generation of the bubble (indicated by the arrow) and the shockwave, which locally mixes the two flows (seen in the white circle).

The last Figure of the sequence shows the final situation, with the generated bubble at the location of the laser spot. By moving the laser slowly, the bubble actually can be displaced within the liquid (not shown in this Figure).

B. Thermal flows for light driven microfluidics

Tuning the optical power, it is possible to find conditions where thermal flows are induced in the microfluidic systems, which can be used to manipulate micrometer sized particles. This was tested in a second series of experiments. **Error! Reference source not found.** explains the general principle. The absorbed radiation in the laser spot leads to local heating. This generates turbulences and convection rolls, which can pull the beads toward the focal spot.
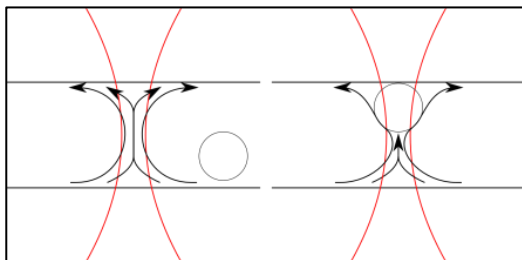

Figure 10. Schematic drawing of the working principle for the manipulation of microbeads: The beads get pulled towards the focal spot due to convection rolls which are caused by the local heating.

Error! Reference source not found. shows snapshots of such an experiment. Polystyrene micro-beads with a diameter of 45 µm were dissolved in a stationary solution of water and ink. When heating the liquid with the laser light, convective flows are generated at the position of the laser spot (see Fig. 10). The beads get attracted towards the focus of the laser spot, which enables the generation of a spot pattern, where each spot features a conglomeration of beads (Fig. 3c). The pattern that we created in this experiment remained in the same position even after the laser was turned off, proving that the beads were moved by the thermal flows, that were generated in the microfluidic chamber by the laser.

Overall these first experiments were successful and confirm the usability of the MOEMS based hardware used in setting up the device. The set-up based on a tunable lens and a micro-mirror provides an efficient and flexible mechanism to steer the laser spot to any position in the working space. Even though, we used rather low laser powers and also the laser spot, in the current set-up, is relatively large, boiling of the liquid and steering of micro beads were achieved easily.
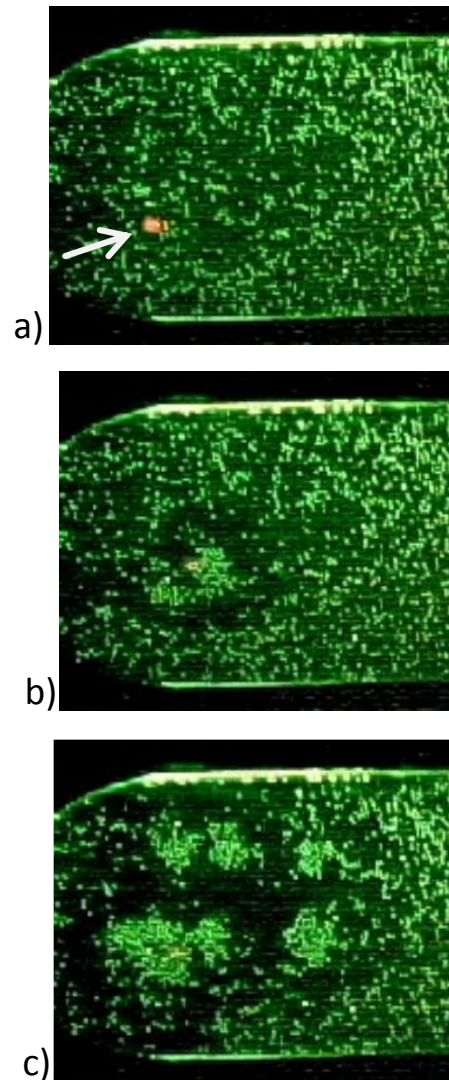

Figure 11. Light-driven manipulation of micro-beads into arranged groups. (a) Image of the laser spot in a homogenous distribution of beads. (b) Beads get pulled towards the position of the laser spot. (c) Formation of a pattern.

V. CONCLUSIONS

In this paper we presented our novel device and showed the results from two proof-of-principle experiments. We demonstrated that the manipulation of microbeads is possible using optically induced thermal flows within a liquid. Furthermore we showed that the generation of bubbles within the liquid is also possible, which leads to the generation of shock waves, which could be used for mixing.

The whole technique is conceptually very simple and relies on relatively simple hardware, since standard diode lasers and focusing optics can be used. At the same time, it enables manipulation of the beads within an unstructured environment, which is a formidable task. Other possible applications, which could be targeted with our scanner device, include the

manipulation of cells as well as the initiation of chemical reactions in microfluidic systems.

REFERENCES

[1] D. Baigl, Photo-actuation of liquids for light-driven microfluidics: state of the art and perspectives, Lab on a Chip 12 (2012) 3637.

[2] M. Blum, M. Büeler, C. Gratzel, and M. Aschwanden, Compact optical design solutions using focus tunable lenses, Optical Design and Engineering, 4 (2011) 81.

[3] V. Milanovic, G. Matus, and D. McCormick, "Gimbal-less monolithic silicon actuators for tip-tilt-piston micromirror applications," IEEE Journal of Selected Topics in Quantum Electronics, 10 (2004) 462.

[4] J. Eichler and H.-J. Eichler, Laser Bauformen, Strahlführung, Anwendungen. Berlin, Heidelberg: Springer-Verlag Berlin Heidelberg, 2010. [Online]. Available: http://dx.doi.org/10.1007/978-3-642-10462-6.